Evidence for an Actin-containing Cytoplasmic Precursor of the Focal Contact and the Timing of Incorporation of Vinculin at the Focal Contact

Joseph A. DePasquale and Colin S. Izzard

Department of Biological Sciences, State University of New York, Albany, New York 12222

Abstract. The distribution of F-actin and vinculin in chicken embryo fibroblasts has been examined by nitrobenzoxadiazol (NBD)-phallacidin and indirect immunofluorescent staining, respectively, and related to the process of focal contact formation by recording the motility of the cell with differential interference contrast (DIC) or interference reflection microscopy (IRM) before fixation for staining. Linear cytoplasmic precursors of the focal contact, present within unattached lamellipodia, stained intensely with NBD-phallacidin. Without exception new focal contacts, 8 s and older at fixation, were associated with either a longer F-actin rib in the lamellipodium or, in older contacts, an F-actin structure of similar dimensions to the contact. This change in distribution of F-actin over the new contacts was accounted for by the segregation of the structural precursor into an attached part over the focal contact and a separate motile part. These results show that F-actin accumulates in the precursor adjacent to areas of the membrane competent to form the focal contact, and are consistent with the interpretation that this F-actin contributes to the initial adhesion plaque associated with the new contact. Vinculin was essentially absent from motile lamellipodia, showed no preferential association with F-actin rich precursors or very young focal contacts, but accumulated over new contacts during a 90-s period. Therefore, the association of F-actin with the membrane that precedes and persists in the initial focal contact is independent of vinculin, and the role of vinculin in development of the focal contact remains unclear.

FIBROBLASTIC cells form two basic types of adhesive cell–substrate contact in culture, the focal and close contact (10). At the light microscope level, the focal contact is invariably associated with a short cytoplasmic fiber of similar shape and size as the contact, or with the distal end of a stress fiber (10–12). At the electron microscope level, a patch of amorphous material, the adhesion plaque, is present at the cytoplasmic face of the focal contact membrane (1), into or through which microfilaments of the stress fiber insert in an, as yet, unclearly defined manner (1, 4, 8). Immunochemical studies have shown that a characteristic set of proteins is concentrated in the cytoplasm at the focal contact, and constitutes part of the adhesion plaque/membrane complex (reviewed in reference 3). Despite this growing body of knowledge, little is known directly about the sequence of events that lead to the structural and molecular organization of the focal contact and associated adhesion plaque/stress fiber complex.

Based on combined differential interference contrast (DIC)[1] and interference reflection microscopy (IRM), the focal contact forms beneath a linear structure in the motile cell margin (11). We have referred to this structure as the cytoplasmic precursor of the focal contact (12). The linear precursors consist of fibers appearing as "ribs" within the motile lamellipodium, or of microspikes or the cores of the latter extending proximally through the lamellipodium. We reasoned that the common structure of the precursor was a bundle of F-actin filaments, based on the interchangeability of the different forms of the precursor (11) and the known ultrastructure of the leading edge (16, 17). This reasoning implied that a preferential accumulation of actin filaments develops adjacent to parts of the membrane competent to form focal contacts before contact is made with the substrate. Others have proposed that the focal contact site develops locally at the cell surface after contact with the substrate by a cooperative accumulation of receptors specific for the focal contact. This leads to the accumulation of vinculin on the cytoplasmic face of the membrane and in turn to the local accumulation of actin filaments (6).

In the present work we sought to (*a*) verify a higher concentration of F-actin in the precursor before contact with the substrate; (*b*) show that F-actin is concentrated over newly formed focal contacts; and (*c*) determine when the accumulation of vinculin begins, relative to formation of the focal contact and its precursor. The activity of the cell margin was

1. *Abbreviations used in this paper*: CEF, chicken embryo fibroblasts; DIC, differential interference contrast; IRM, interference reflection microscopy; NBD-phallacidin, nitrobenzoxadiazol-phallacidin.

© The Rockefeller University Press, 0021-9525/87/12/2803/7 $2.00

recorded before fixation to identify motile precursors by DIC, or unattached lamellipodia and new focal contacts by IRM. Then the distribution of F-actin and vinculin was examined in the same cell by nitrobenzoxadiazol-phallacidin (NBD-phallacidin) staining (2) and indirect immunofluorescence, respectively. Preliminary reports of parts of this work have been given (5, 12).

Materials and Methods

Cell Culture

Cultures of chicken embryo fibroblasts (CEF) were prepared from 9–11 d-old embryos and maintained in DME (Gibco, Grand Island, NY) supplemented with 10% FBS (Flow Laboratories, Inc., McLean, VA), nonessential amino acids (Gibco), and 50 U/ml penicillin and 50 μg/ml streptomycin (Gibco). Cells were not used for experiments past the fifth passage. For microscopy, cells were seeded on coverslips and used within 24 h. Coverslips were inverted on spacers and sealed along two sides leaving two ends open as a simple perfusion chamber. The preparations were maintained at 37°C on the microscope with an air-curtain incubator (Sage Instruments Div., Orion Research Inc., Cambridge, MA). The motile history of an individual cell was recorded, and the cell fixed and processed for fluorescent staining by perfusion through the chamber while on the microscope.

Light Microscopy and Video Recording

A microscope (Universal Scientific, Inc., Atlanta, GA), equipped with III RS vertical illuminator, diaphragm aperture insert, and 100/1.25 planachromat oil-immersion objective lens (Carl Zeiss, Inc., Thornwood, NY), was used for fluorescence, DIC, and IRM. The selective exciter-barrier filter/dichroic mirror combinations (catalogue Nos. 487717 and 487715; Carl Zeiss Inc.) were used to observe and separate the fluorescence from the NBD- and TRITC-labeled probes, respectively. A half-surface plane-glass mirror, and neutral glass plate in the barrier-filter position, were inserted in the III RS illuminator and used for IRM.

The DIC images were recorded via a Newvicon video camera (67M; Dage-MTI, Inc., Michigan City, IN) and the associated fluorescence with an ISIT video camera (66 ISIT; Dage-MTI, Inc.). The IRM images and associated fluorescence were both recorded via the ISIT camera to ensure matching geometry in the images. Images from the ISIT camera were noise-reduced in real-time by recursive frame-averaging using an Intellect 100 image processor (MCI Quantel, Micro Consultants Inc., Palo Alto, CA) and a shift factor of 1 for live IRM and 5–7 for fixed fluorescent images. The ISIT camera was operated mostly in the automatic mode. However, in areas of the specimen where the fluorescent intensity showed little amplitude modulation or was weak, the video image was analogue enhanced by increasing the gain of the camera in the manual mode, or digitally enhanced using the integration function of the image processor. No localized fluorescence, beyond that seen with the camera in the automatic mode, was detected by the two enhancement methods.

The video images were mixed with a time-base, providing video-field number (model 346; Thalner Electronics Lab., Inc., Ann Arbor, MI), and recorded with a 1/2-inch VCR (model 8050; Panasonic Co., Secaucus, NJ). The motile history of individual live cells and the process of fixation were recorded at a time-lapse rate of every twelfth video-field. Subsequent processing and the final fluorescent images were recorded at the normal video-frame rate. Noise-reduced images from successive planes of focus through the fluorescent specimens were recorded on the tapes. The horizontal resolution was 400 TV lines for the ISIT camera, and 320 TV lines for the VCR.

Video images were photographed from the monitor (model EVM 1220; Electroholme, Kitchener, Ontario, Canada) and the negatives overlaid to determine the spatial correspondence of F-actin or vinculin-containing structures with each other, and with focal contacts or cytoplasmic precursors. Conventional 35-mm photomicrographs of the fluorescent images were taken on a Photomicroscope II (Carl Zeiss, Inc.), and compared with those obtained from the same cell with the ISIT camera after noise reduction, recording on tape, and replay on the monitor.

Fixation and Fluorescent Staining

In all experiments, the cells were fixed first and then permeabilized with detergent before staining to avoid loss of protein from structures of interest, with the exception of one set that was extracted first with detergent to evaluate the origin of diffuse vinculin staining and its effect on the detection of weak localized staining.

Cells in culture medium were perfused directly with 2% glutaraldehyde in 0.1 M cacodylate buffer, pH 7.4, at 37°C and fixed for 5 min. Subsequent steps were carried out in the same buffer at 23°C. The cells were washed with buffer, permeabilized with 0.5% Triton-X 100 for 1 min, treated with 0.1 M glycine for 10 min, washed in buffer, and then incubated with NBD-phallacidin (Molecular Probes, Inc., Junction City, OR) for 20 min. NBD-phallacidin was used at 40–100 ng/100 μl, depending upon the lot used. The optimal concentration for each lot was determined by staining and bleaching the cells, and then testing whether the bleached cells could be restained. After staining, the cells were washed and the fluorescence observed in buffer.

For vinculin staining, cells were fixed for 5 min at 37°C with 3.7% paraformaldehyde in the low calcium, buffered salt solution of Small (16), pH 7.2. Subsequent steps were at 23°C and used this buffer. The fixed cells were permeabilized with 0.5% Triton-X 100 for 20 min, treated with 0.1 M glycine for 10 min, and washed with buffer. The cells were incubated with guinea pig anti-vinculin serum (1:25 dilution) and then TRITC-conjugated goat anti-guinea pig IgG (1:60 dilution) (Cappel Laboratories, Cochranville, PA) for 10 min, each in the presence of 0.1% Tween 20, which significantly reduced the diffuse background fluorescence, but did not reduce the discrete localized fluorescence in the cells. The guinea pig anti-vinculin serum previously had been shown to be monospecific for the immunogen (15). Controls using preimmune guinea pig serum were negative. In double labeling experiments, NBD-phallacidin was applied before the antibodies.

Results

Actin Content and Attachment of Cytoplasmic Precursors

Cytoplasmic precursors consisting of fibers within the breadth of the lamellipodium, or microspikes and their cores extending into the lamellipodium are shown in Fig. 1, *A*, *D*, *E*, and *F* (*arrowheads*). They lie within the plane of focus of the lamellipodium, and are distinguishable from and do not represent optical sections of radial folds or pleats in the lamellipodium. Without exception, the precursors stained more intensely for F-actin than the adjacent lamellipodium (Fig. 1, *G*, and *I*, *matched arrowheads*). Similar intensely stained ribs were present in motile, unattached lamellipodia identified by IRM (Fig. 2, *D* and *E*, *double arrowheads*).

Attachment of the cytoplasmic precursor to the substrate could be followed in the DIC-video records of the live cells. For example, the proximal part of the motile precursor in Fig. 1 *A* (*arrow*) became stationary (Fig. 1, *B–F*) and persisted as the adhesion plaque associated with a focal contact (Fig. 1, *G* and *H*, *arrows*). The distal part of the precursor separated from the proximal part (Fig. 1, *C* and *D*) and then elongated within the lamellipodium to reconstitute a typical precursor (Fig. 1 *E*). Both parts of the original precursor stained strongly for F-actin (Fig. 1, *G* and *I*, *arrows* and *double arrowheads*). In all cases examined, the origin of adhesion plaques in the leading lamella was traced to the attachment and segregation of the proximal part of a motile cytoplasmic precursor. The segregation was not observed in motile precursors and therefore occurs specifically in response to contact with the substrate.

Frame-by-frame analysis of the DIC-video records showed that there was no decrease in contrast in the image of the proximal part of the precursor during its attachment and segregation from the distal part (e.g., between Fig. 1, *C* and *D*). In addition, segregation of the precursor into two parts did not involve a longitudinal splitting of the adherent seg-

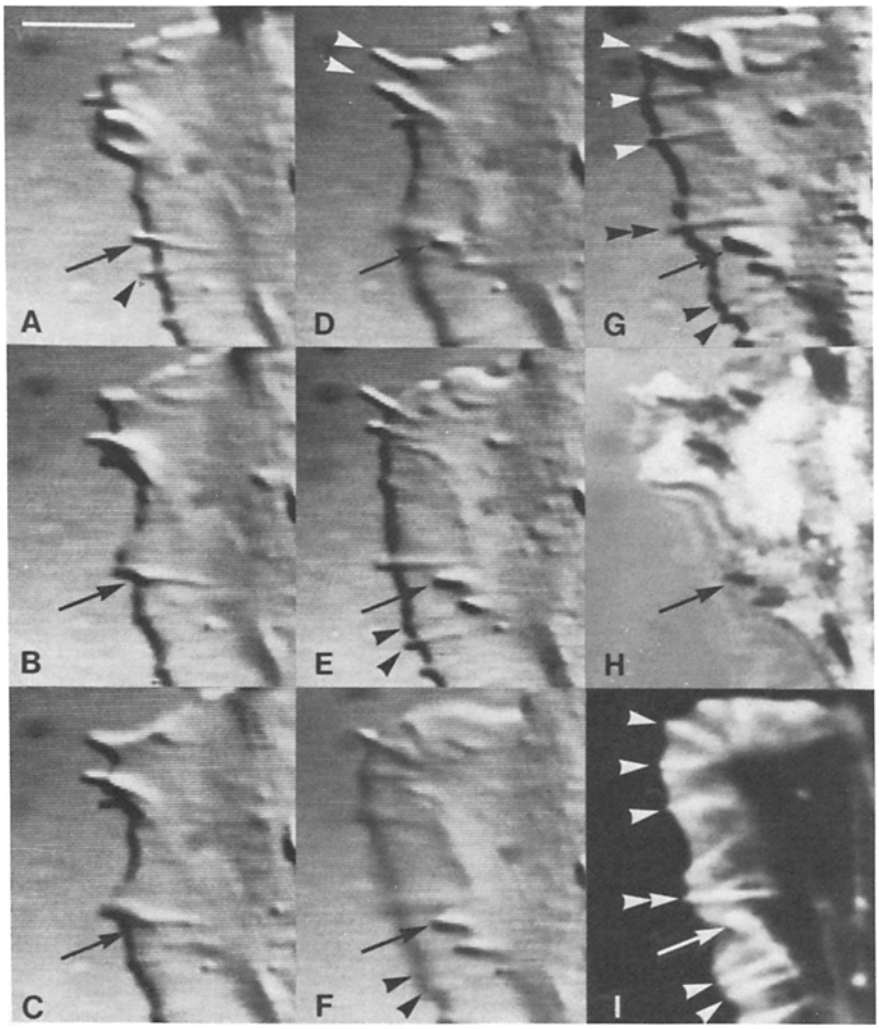

Figure 1. F-actin distribution in the motile cell margin of a CEF. (*A–F*) DIC-video records of live cell. Time before fixation (min:s): (*A*) 2:00; (*B*) 1:40; (*C*) 1:30; (*D*) 1:15; (*E*) 0:30; (*F*) 0:01. (*G–I*) The same cell after fixation with 3.7% paraformaldehyde in Small's buffer: (*G*) DIC; (*H*) IRM; (*I*) NBD-phallacidin fluorescence. In the live cell, cytoplasmic precursors of the focal contact (*A, D, E, F, arrowheads*) are present within the lamellipodium, which advances (*A–F*) and lifts away from the substrate together with the contained precursors (*E* and *F, matched arrowheads*). Individual precursors are preserved by fixation (*G, arrowheads*) in the lamellipodium, which is not in contact with the substrate (*H*). Each precursor stained intensely with NBD-phallacidin (*G* and *I, matched arrowheads*) within the band of fluorescence corresponding to the lamellipodium. The live-cell sequence also shows the attachment of a motile precursor (*A, arrow*) to the substrate. The proximal part of the precursor became stationary, thickened, and persisted as a short structure at the substrate level (*B–F, matched arrows*). After fixation, the structure coincided with a focal contact and stained intensely with NBD-phallacidin (*G, H, I, matched arrows*). The part of the precursor distal to the arrow-point curved away (*B, C*), separated from the proximal attached part (*D*), and then elongated within the lamellipodium (*E*). The elongated fiber stained intensely with NBD-phallacidin (*G, I, double arrowheads*), but was not in contact with the substrate (*H*). Bar, 5 μm.

ment or complete peeling of the cytoplasmic rib from the membrane in cases where the tip moved laterally and such events would be detectable in the plane of optical section (e.g., Fig. 1, *B–D*). Therefore, by these two criteria, the bulk of the structure of the proximal part of the precursor is retained as the initial adhesion plaque.

Actin Association with New Focal Contacts

The high concentration of F-actin in the cytoplasmic precursor and the structural segregation of the precursor imply that a similar high concentration of F-actin will be present over new focal contacts from the beginning. This implication was tested by examining the distribution of NBD-phallacidin staining associated with new focal contacts of known age. The cells were fixed with glutaraldehyde (see Materials and Methods), which preserved all new substrate contacts. Each new contact, including a significant number <30-s old, was present beneath an elongate region of intense fluorescence in the NBD-phallacidin stained cell (Table I, A). The youngest contact examined was 8-s old at fixation.

Two-thirds of the new contacts were first detected under the lamellipodium. About one-third still remained under the otherwise motile lamellipodium at fixation (Table II, A), and typically were present beneath a segment of a longer overlying fluorescent rib in the lamellipodium (Fig. 2, *D* and *E, matching arrows*). The remainder of the focal contacts was located within the close contact or at its boundary at fixation (Table II, A). In these cases, the fluorescent area coincided more exactly with that of the contact, e.g., as shown in Fig. 1, *H* and *I, arrows*. This change in distribution of the F-actin associated with the new contacts is consistent with the structural segregation of the cytoplasmic precursor and retention of its proximal part as the initial adhesion plaque (Fig. 1, *A–F*). There was no obvious decrease in the staining for F-actin associated with the new contacts in any of the successive age groups in Table I, A, nor for the contacts no longer under the lamellipodium at fixation. The persistent staining suggests that F-actin in the precursor is retained as a component of the adhesion plaque as the contact forms.

Thin fibers staining weakly with NBD-phallacidin extended from some of the older contacts into the cell (Fig. 2, *D* and *E, matching arrowheads*). However, within the timeframe of these studies, large stress fibers intensely stained with NBD-phallacidin and extending centripetally from the new contacts into the cell were not developed.

Table I. Age Distribution of New Focal Contacts at Fixation (No. of Contacts)

	Age (s)								
	0–30	31–60	61–90	91–120	121–150	151–180	181–210	211–240	241–270
A Cells stained with NBD-phallacidin	21	37	26	21	9	6	1	–	–
B Cells stained with anti-vinculin	19	26	13	9	3	2	4	1	3
C Level of vinculin staining for (B)									
Vn−	6	3	0	0	0	0	0	0	0
Vn+	8	13	4	0	1	0	0	1	0
Vn++	5	8	9	6	1	1	2	0	2
Vn+++	0	2	0	3	1	1	2	0	1

The motility of individual cells was recorded using IRM, and the age at fixation of all the new focal contacts determined.
Part A: Data from 34 cells stained only with NBD-phallacidin. All the new contacts were strongly stained (see text).
Part B: Data from 14 cells stained with anti-vinculin, five of which were also stained with NBD-phallacidin.
The duration of the video records before fixation ranged from 2 to 4 min for the cells in A, and from 2 to 7 min for the cells in B, which accounts for the larger number of new contacts in the younger age groups.
Part C: The age distribution of the new contacts in the cells stained with anti-vinculin (Part B) is tabulated for different levels of vinculin staining associated with the contacts. Vn−, contact unstained; Vn+, contact very weakly stained in spots; Vn++, contact area weakly and uniformly stained; Vn+++, contact area uniformly and strongly stained.

Vinculin Accumulation

Vinculin was essentially absent from unattached lamellipodia (Fig. 2, *D* and *F*). It was not preferentially accumulated over the F-actin in the cytoplasmic precursors in the lamellipodium (Fig. 2 *E*, *double arrowheads*, and *F*). Vinculin accumulated after the focal contact formed. For example, each of the three new contacts in Fig. 2 coincided with a segment of an F-actin rich rib in the lamellipodium, but one did not stain for vinculin and two stained weakly compared with other contacts. Accumulation of vinculin at the contact was progressive. Approximately 10% of the contacts examined were completely unlabeled for vinculin and mostly <30-s old (Table I, C, Vn−). Very weak staining, often as a cluster of spots (Fig. 2 *F*, *arrow 2*), was typical of contacts <60-s old (Table I, C, Vn+). Strong staining for vinculin (Fig. 2, *D* and *F*, *arrowheads*), comparable to that in large older contacts, was present primarily in contacts >90-s old (Table I, C, Vn+++).

Table II. Location of Focal Contacts at Time of Formation and Fixation (No. of Contacts)

	Location of focal contact				Total new contacts
	MS	LP	CC/LP	CC	
A Cells stained with NBD-phallacidin					
At formation	13	81	22	5	121
At fixation	0	36	57	28	121
B Cells stained with anti-vinculin					
At formation	0	82	4	1	87
At fixation	0	44	25	18	87
C Level of vinculin staining for (B)					
Vn−	0	7	2	0	9
Vn+	0	16	9	2	27
Vn++	0	20	8	9	37
Vn+++	0	1	6	7	14

The motility of individual cells was recorded using IRM, and the location of all new contacts determined when first formed and at the time of fixation. Location of focal contacts: MS, under microspike; LP, under lamellipodium; CC/LP, at boundary of close contact and lamellipodium; CC, within close contact. See Table I for details of cells and explanation of level of vinculin staining.

The level of accumulation of vinculin over new focal contacts was also related to the location of the contact at the time of fixation. Significantly, contacts not stained for vinculin were still under the lamellipodium (Table II, C, Vn−) where most were first formed (Table II, B). Other contacts still under the lamellipodium were only weakly stained for vinculin (Table II, C, Vn+, Vn++). The strongly stained contacts were within the close contact area or at its boundary (Table II, C, Vn+++). Therefore, accumulation of vinculin can begin while the contact remains under the otherwise motile lamellipodium, and continues as the close contact advances relative to the stationary focal contact.

Fluorescent images of the vinculin distribution were recorded directly by conventional 35-mm photomicrography and compared with those obtained subsequently from the same cell with the ISIT camera in the automatic mode, after noise reduction, recording on tape, and replay on the monitor. We were concerned (*a*) that weakly fluorescent structures would not be detected because of the limited intrascene dynamic range of the video camera, and (*b*) that structural detail would be lost because of the limited resolution of the ISIT camera and video recorder. As predicted, the relative intensity, and therefore contrast, of the weaker background fluorescence was lower, and the sharpness of the granularity in the background less in images recorded by the video system than by conventional photography (Fig. 3, *A* and *B*). Nevertheless, the same fluorescent structures could be identified in both images. Contrast in the areas of background fluorescence was routinely analogue enhanced by increasing the gain of the camera in the manual mode, but no

Table I. Continued

271–300	301–330	331–360	361–390	Total new contacts
–	–	–	–	121
1	2	3	1	87
0	0	0	0	9
0	0	0	0	27
0	0	2	1	37
1	2	1	0	14

additional localized fluorescence demonstrated. Some live cells were extracted briefly with 0.5% Triton-X 100 in Small's buffer before fixation. The diffuse intracellular vinculin staining was reduced, but not eliminated, suggesting that it represented in part a soluble pool of vinculin. The preextraction did not remove vinculin associated with focal contacts, or reveal any patches of vinculin otherwise masked by the diffuse staining in prefixed cells.

Discussion

In this study, we have shown that F-actin is concentrated in the linear cytoplasmic precursor of the focal contact and in the adhesion plaque associated with the newly formed focal contact in CEF. In contrast, vinculin is absent from the cytoplasmic precursor, but accumulates progressively over the focal contact and therefore in the presence of F-actin.

These results differ significantly from steps in the model proposed by Geiger et al. (6) for focal contact formation. These authors proposed that, after initial attachment of the cell to the substrate through a variety of receptors, cell surface receptors specific for the focal contact aggregate locally, in a positively cooperative fashion, to form an adhesive patch. This aggregation is proposed to initiate the binding of vinculin to the inner side of the membrane, which in turn leads to the organization of filamentous actin into bundles of uniform polarity. Geiger et al. (6) state that their model predicts the association of vinculin with the membrane before actin. However, we have found no evidence to support this prediction. Instead we have documented the accumula-

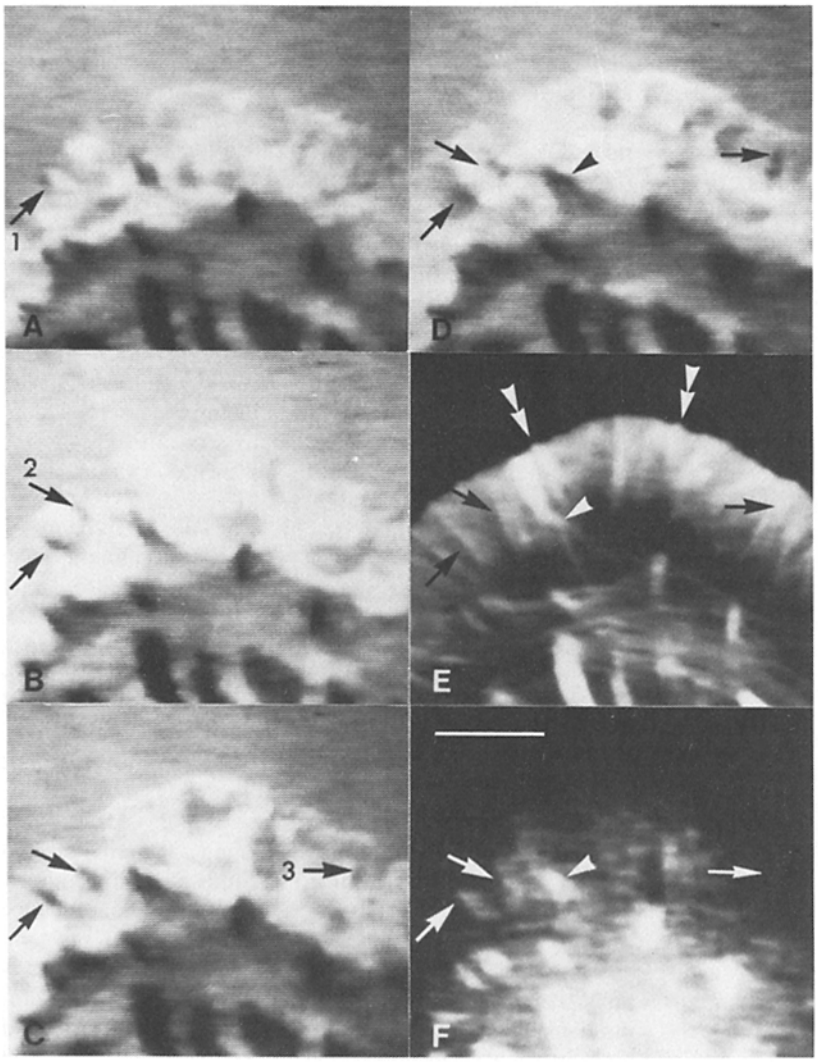

Figure 2. Association of actin and vinculin with focal contacts of known age in the cell margin of a CEF. (*A–D*) IRM-video records of live cell. Time before fixation (min:s): (*A*) 1:13; (*B*) 0:54; (*C*) 0:24; (*D*) 0:05. (*E–F*) The same cell after fixation with 3.7% paraformaldehyde in Small's buffer: (*E*) NBD-phallacidin fluorescence; (*F*) indirect immunofluorescent staining for vinculin. In the IRM images of the live cell, the lamellipodium appears as a brighter mottled band extending ahead of the darker close contact (*A–D*). A row of focal contacts at the margin of the close contact (*A*) were present before the video recording began, and stained for F-actin (*E*) and vinculin (*F*). Three new focal contacts, marked by numbered arrows in *A*, *B*, and *C* and followed by matching arrows, formed under the lamellipodium and, after fixation, each coincided with part of an F-actin rich rib in the lamellipodium (*E*). Focal contacts *1* and *2* stained weakly, but focal contact *3* was unstained for vinculin (*F*). The age of contacts *1*, *2*, and *3* at fixation was 1:15, 0:56, and 0:48 (min:s), respectively. Other F-actin rich ribs (*E*, *double arrowheads*) were not attached to the substrate (*D*) and did not stain for vinculin (*F*). The focal contact marked by a single arrowhead in D was 4:19 (min:s) old at fixation and stained for F-actin and strongly for vinculin (*E*, *F*, *matching arrowheads*). Bar, 5 μm.

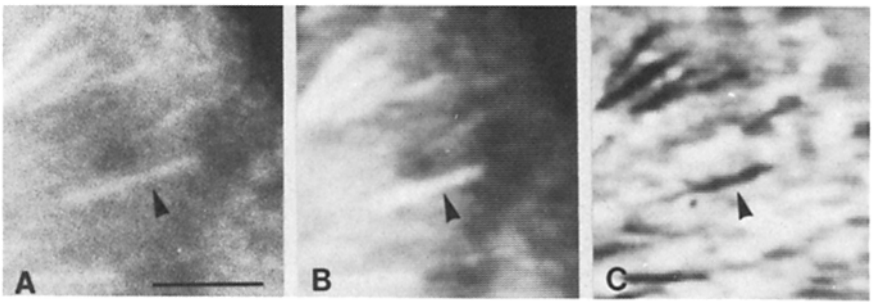

Figure 3. (*A–B*) Indirect immunofluorescent staining for vinculin in cell margin of a CEF. (*C*) IRM of same area. Cell fixed with 3.7% paraformaldehyde in Small's buffer and then permeabilized with detergent. (*A*) Direct 35-mm photomicrograph of fluorescent image; (*B*) the same image subsequently recorded with the ISIT video camera, noise reduced, recorded on tape, and photographed after replay from the monitor. (*C*) Similarly derived video-IRM image. In the cell margin (*top right*), the contrast and sharpness of the granularity in the weak background fluorescence are less in the video image (*B*) than in the direct photograph (*A*). No additional fluorescent structures are present in the direct photograph. However, the contrast of the vinculin staining associated with focal contacts (*matching arrowheads*) is significantly greater in the video image (*B*). Bar, 5 μm.

tion of vinculin at the contact in the presence of F-actin. Furthermore, our data suggest that this actin is derived from the precursor. Therefore, vinculin cannot play a role in the initial organization of actin at the contact.

Formation of the focal contact beneath an F-actin rich cytoplasmic precursor implies that the cell surface of the unattached precursor possesses the adhesive properties required to form the contact. This raises another difference from the model of Geiger et al. (6), in which it is proposed that receptors specific for the contact aggregate locally after attachment of the cell to the substrate. The idea that the cell surface of the motile precursor is predifferentiated is supported by the very rapid formation of the focal contact (in <1 s) as a stable adhesion versus the slow development of the close contact which often remains labile for up to 60 s (11).

The structural segregation of the precursor and persistent staining of new contacts for F-actin suggest that part of the F-actin in the unattached precursor is retained as a component of the initial adhesion plaque. This transfer of actin filaments from precursor to plaque does not conflict with the known dynamics of actin in this region of the cell. For example, fluorescent recovery after photobleaching experiments show little exchange of actin along the length of the precursor, or in the adjacent lamellipodium, during a 4–7-min period (22). Similarly, ~80% of the actin over focal contacts and in stress fibers exchanges with a half-time of 10 min (13). Therefore, actin filaments present before and after contact are stable relative to the time course for attachment and segregation of the precursor, i.e., ~30 s in Fig. 1, *B–D* and up to 90 s in other examples. Moreover, the treadmilling of actin subunits along the precursor filaments, inferred from the pattern of fluorescence recovery, occurs at 0.79 μm/min (22), and it would take 4–6 min for the actin in a precursor, 3–5-μm long, to totally exchange by this means. These exchange studies show that it is possible for the filaments to persist long enough to be transferred to the adhesion plaque. Nevertheless, different conditions could be present at the time, and it will be important to study the exchange of actin directly during this period.

The structure of the precursor at the electron microscopic level also is consistent with the transfer of F-actin to the contact. However, the ultrastructure raises some interesting questions about how this is fully effected. Many individual filaments extend to the tip of the F-actin bundle of the precursor and terminate in patches of material thought to be derived from the plasma membrane (9, 14, 20). Other filaments converging from the lamellipodium into the bundle appear to terminate along its length at patches of material similar to that at the tip (9, 14). Therefore, an end-on insertion of filaments at the membrane also appears to be present in the precursor where the focal contact actually forms, and could account for the retention of these filaments at the contact. The terminations of other filaments within the length of the bundle are unclear (9, 14, 20). Our data suggest that the bulk of these filaments is also retained at the focal contact rather than peeling away from the adherent membrane or immediately disassembling. This raises the question of whether the more central filaments are severed transversely or rearranged, and whether the filaments are retained through existing crosslinks or by insertion at the membrane.

Small and co-workers report a marked association between the position of vinculin foci in fixed cells and sites of "ruffling" activity in live cells. They conclude that ruffling, like microspike protrusion, also precedes and therefore predetermines the site of contact (18, 19). However, we would argue against their conclusion as follows. They used only phase-contrast microscopy to document the motile history of the cell margin, and direct information on the timing of contact formation in the live cell is lacking. They also report the presence of vinculin foci in the absence of ruffling under lamellipodia and microspikes (7). The cytoplasmic fibers seen in the lamellipodium by DIC (Fig. 1), and the bundles of actin filaments shown by them to be present in the cell margin at the electron microscopic level (16, 20), are barely detectable, if at all, in their phase-contrast images (7, 18, 19), and they may have missed the correlation between the F-actin rich precursors and subsequent localization of vinculin described in this work. Furthermore, they state that the radial form of ruffle contains one or more actin-rich bundles, i.e., equivalent to the precursors described here. Also, their phase-dark mini-ruffles are remarkably similar in size, shape, and location to the adhesion plaques (Fig. 1, *G* and *H*, *arrow*), the origin of which from the F-actin containing precursors can be followed clearly in DIC optics. In this context, we suggest that the "ruffling" activity may be a consequence rather than a determinant of contact formation.

We have concentrated on some of the events that immediately precede and follow contact formation. However, the focal contact subsequently increases several-fold in area and there is a related increase in the size of the adhesion plaque

(11). Also, the number of filaments inserting at the contact increases (1, 8), and stress fibers develop centripetally from the plaque into the cell (11, 21). What role vinculin plays, together with other proteins, in the maturation of the adhesion plaque/focal contact complex, or in the development of stress fibers, is unclear at present. Therefore, further time-resolved studies of the changes in structure and protein composition that occur during development and attachment of the precursor, and after formation of the focal contact, are being conducted to resolve these and other questions.

We are indebted to Dr. I. I. Singer, Merck, Sharp and Dohme Research Laboratories, Rahway, NJ, for his generous gift of the guinea pig anti-vinculin serum and the preimmune serum.

This investigation was supported by U.S. Public Health Service grant number CA32829, awarded by the National Cancer Institute, Department of Health and Human Services, and National Science Foundation grant number DCB-8702511, to C. S. Izzard.

Received for publication 12 May 1987, and in revised form 18 August 1987.

References

1. Abercrombie, M., J. E. M. Heaysman, and S. M. Pegrum. 1971. The locomotion of fibroblasts in culture. *Exp. Cell Res.* 67:359–367.
2. Barak, L. S., R. R. Yocum, E. A. Nothnagel, and W. W. Webb. 1980. Fluorescence staining of the actin cytoskeleton in living cells with 7-nitrobenz-2-oxa-1,3 diazole-phallacidin. *Proc. Natl. Acad. Sci. USA.* 77:980–984.
3. Burridge, K. 1986. Substrate adhesions in normal and transformed fibroblasts: organization and regulation of cytoskeletal, membrane and extracellular matrix components at focal contacts. *Cancer Rev.* 4:18–78.
4. Chen, W.-T., and S. J. Singer. 1982. Immunoelectron microscopic studies of the sites of cell-substratum and cell-cell contacts in cultured fibroblasts. *J. Cell Biol.* 95:205–222.
5. DePasquale, J. A., and C. S. Izzard. 1985. Evidence for an actin-containing cytoplasmic precursor of the focal contact. *J. Cell Biol.* 101:411a. (Abstr.)
6. Geiger, B., Z. Avnur, T. E. Kreis, and J. Schlessinger. 1984. The dynamics of cytoskeletal organization in areas of cell contact. *Cell Muscle Motil.* 5:195–234.
7. Geiger, B., Z. Avnur, G. Rinnerthaler, H. Hinssen, and J. V. Small. 1984. Microfilament-organizing centers in areas of cell contact: cytoskeletal interactions during cell attachment and locomotion. *J. Cell Biol.* 99: 83s–91s.
8. Heath, J. P., and G. A. Dunn. 1978. Cell to substratum contacts of chick fibroblasts and their relation to the microfilament system. A correlated interference-reflexion and high-voltage electron-microscope study. *J. Cell Sci.* 29:197–212.
9. Höglund, A. S., R. Karlsson, E. Arro, B.-A. Fredriksson, and U. Lindberg. 1981. Visualization of the peripheral weave of microfilaments in glia cells. *J. Musc. Res. Cell Motil.* 1:127–146.
10. Izzard, C. S., and L. R. Lochner. 1976. Cell-to-substrate contacts in living fibroblasts: an interference reflexion study with an evaluation of the technique. *J. Cell Sci.* 21:129–159.
11. Izzard, C. S., and L. R. Lochner. 1980. Formation of cell-to-substrate contacts during fibroblast motility: an interference-reflexion study. *J. Cell Sci.* 42:81–116.
12. Izzard, C. S., S. L. Izzard, and J. A. DePasquale. 1985. Molecular basis of cell-substrate adhesions. *Exp. Biol. Med.* 10:1–22.
13. Kreis, T. E., B. Geiger, and J. Schlessinger. 1982. Mobility of microinjected rhodamine actin within living chicken gizzard cells determined by fluorescence photobleaching recovery. *Cell.* 29:835–845.
14. Lindberg, U., A. S. Höglund, and R. Karlsson. 1981. On the ultrastructural organization of the microfilament system and the possible role of profilactin. *Biochimie.* 63:307–323.
15. Singer, I. I., and P. R. Paradiso. 1981. A transmembrane relationship between fibronectin and vinculin (130 kd protein): serum modulation in normal and transformed hamster fibroblasts. *Cell.* 24:481–492.
16. Small, J. V. 1981. Organization of actin in the leading edge of cultured cells: influence of osmium tetroxide and dehydration on the ultrastructure of actin meshworks. *J. Cell Biol.* 91:695–705.
17. Small, J. V., G. Isenberg, and J. E. Celis. 1978. Polarity of actin at the leading edge of cultured cells. *Nature (Lond.).* 272:638–639.
18. Small, J. V., and G. Rinnerthaler. 1985. Cytostructural dynamics of contact formation during fibroblast locomotion in vitro. *Exp. Biol. Med.* 10: 54–68.
19. Small, J. V., G. Rinnerthaler, Z. Avnur, and B. Geiger. 1985. Cytoarchitectural changes associated with fibroblast locomotion: involvement of ruffling and microtubules in the establishment of new substrate contacts at the leading edge. *In* Contractile Proteins in Muscle and Nonmuscle Systems. Biochemistry, Physiology and Pathology. M. A. Russo, editor. Praeger, New York. 363–381.
20. Small, J. V., G. Rinnerthaler, and H. Hinssen. 1982. Organization of actin meshworks in cultured cells: the leading edge. *Cold Spring Harbor Symp. Quant. Biol.* 46:599–611.
21. Wang, Y.-L. 1984. Reorganization of actin filament bundles in living fibroblasts. *J. Cell Biol.* 99:1478–1485.
22. Wang, Y.-L. 1985. Exchange of actin subunits at the leading edge of living fibroblasts: possible role in treadmilling. *J. Cell Biol.* 101:597–602.